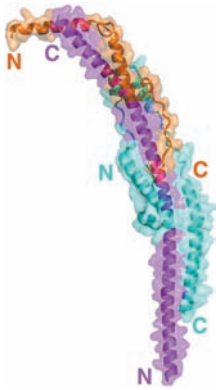

Figure 22-40 **X-ray structure of a portion of the peripheral stalk of bovine F_1F_0–ATPase.** This protein fragment is drawn in ribbon form embedded in its semitransparent molecular surface, with *b* (residues 79–183) magenta, *d* (residues 3–123) cyan, and F_6 (residues 5–70) orange. The N- and C-termini of each subunit are indicated. [Based on an X-ray structure by Andrew Leslie and John Walker, MRC Laboratory of Molecular Biology, Cambridge, U.K. PDBid 2CLY.]

site, thereby conferring an hourglasslike shape on the c_{11} assembly (Fig. 22-39*a*). Each Na^+ ion is liganded by residues from both helices of a given subunit as well as those of the clockwise neighboring outer helix as seen in Fig. 22-29*b*.

In vertebrates, the peripheral stalk (Fig. 22-37) consists of the OSCP, *b, d,* and F_6 subunits, whereas in most prokaryotes, it consists of the OSCP homolog δ and two copies of *b*. The X-ray structure of most of the cytosolic portion of a complex of bovine subunits *b, d,* and F_6, constituting 54% of the extramembrane segment of the peripheral stalk, determined by Leslie and Walker, reveals that this *b* fragment forms a 160-Å-long and curved α helix, and that the other subunit fragments are also mainly helical (Fig. 22-40). The curvature of this assembly closely matches that of the peripheral stalk in cryoEM-based images of the F_1F_0–ATPase (e.g., Fig. 22-37). Such cryoEM-based images, together with the foregoing X-ray structures and the NMR structures of δ and the transmembrane segment of *b,* both from *E. coli,* has enabled the construction of a composite model of the *E. coli* F_1F_0–ATPase (Fig. 22-41), which, of course, resembles the mitochondrial assembly. Note the extensive contacts between γ and ε and the top of the *c* cylinder.

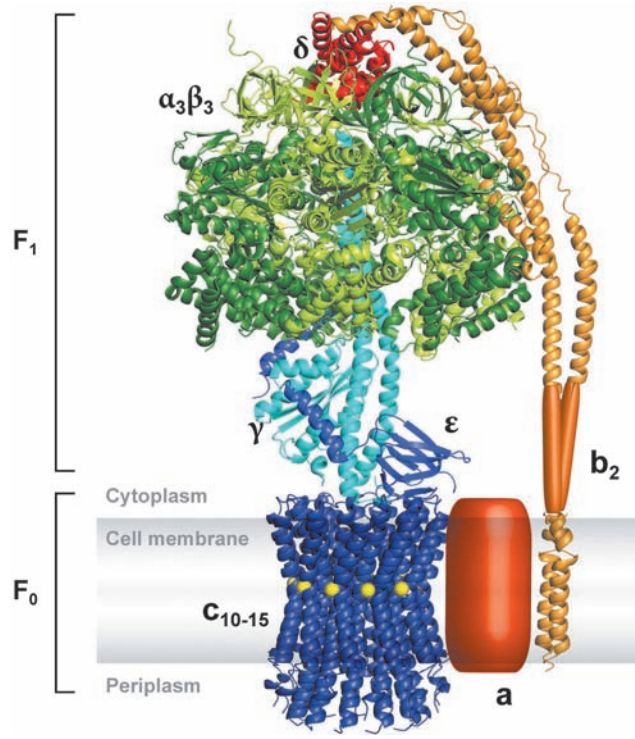

Figure 22-41 **A composite model of the *E. coli* F_1F_0–ATPase.** This model is based on the X-ray structure of the *E. coli* F_1 subunit (PDBid 1JNV), which resembles that of bovine F_1 (Fig. 22-38), the structures displayed in Figs. 22-39 and 22-40, and the NMR structures of δ and the transmembrane segment of the *b* from *E. coli* (PDBids 2A7U and 1B9U). The structures of *a* and the so-called hinge region of *b* are unknown. [Courtesy of Peter Dimroth, ETH, Zürich, Switzerland.]

d. The Binding Change Mechanism: Proton-Translocating ATP Synthase Is Driven by Conformational Changes

The mechanism of ATP synthesis by proton-translocating ATP synthase can be conceptually broken down into three phases:

1. Translocation of protons carried out by F_0.

2. Catalysis of formation of the phosphoanhydride bond of ATP carried out by F_1.

3. Coupling of the dissipation of the proton gradient with ATP synthesis, which requires interaction of F_1 and F_0.

The available evidence supports a mechanism for ATP formation, proposed by Boyer, that resembles the conformational coupling hypothesis of oxidative phosphorylation (Section 22-3A). However, the conformational changes in the ATP synthase that power ATP formation are generated by proton translocation rather than by direct electron transfer, as proposed in the original formulation of the conformational coupling hypothesis.

F_1 is proposed to have three interacting catalytic protomers, each in a different conformational state: one that binds substrates and products loosely (L state), one that binds them tightly (T state), and one that does not bind them at all (open or O state). The free energy released on proton translocation is harnessed to interconvert these three states. The phosphoanhydride bond of ATP is synthesized only in the T state and ATP is released only in the O state. The reaction involves three steps (Fig. 22-42):

1. Binding of ADP and P_i to the "loose" (L) binding site.

2. A free energy–driven conformational change that converts the L site to a "tight" (T) binding site that catalyzes the formation of ATP. This step also involves conformational changes of the other two subunits that convert

LHC	light-harvesting complex
LT	leukotriene
LX	lipoxin
MALDI	matrix-assisted laser desorption/ionization
Man	mannose
MAPK	mitogen-activated protein kinase
Mb	myoglobin
MHC	major histocompatability complex
miRNA	microRNA
MKK	MAP kinase kinase
mRNA	messenger RNA
MS	mass spectrometry
MurNAc	*N*-acetylmuramic acid
NA	neuraminidase
NAD^+	nicotinamide adenine dinucleotide, oxidized form
NADH	nicotinamide adenine dinucleotide, reduced form
$NADP^+$	nicotinamide adenine dinucleotide phosphate, oxidized form
NADPH	nicotinamide adenine dinucleotide phosphate, reduced form
NAG	*N*-acetylglucosamine
NAM	*N*-acetylmuramic acid
NANA	*N*-acetylneuraminic (sialic) acid
NDP	nucleoside diphosphate
NEM	*N*-ethylmaleimide
NER	nucleotide excision repair
NeuNAc	*N*-acetylneuraminic acid
NMN	nicotinamide mononucleotide
NMR	nuclear magnetic resonance
NOESY	nuclear Overhauser effect spectroscopy
NOS	nitric oxide synthase
NRK	nonreceptor tyrosine kinase
NSAID	nonsteroidal anti-inflammatory drug
NSF	NEM-sensitive fusion protein
NTP	nucleotide triphosphate
OEC	oxygen-evolving complex
OMP	orotidine monophosphate
ORF	open reading frame
P or p	phosphate
P_i	orthophosphate ion
PAGE	polyacrylamide gel electrophoresis
PAP	poly(A) polymerase
PBG	porphobilinogen
PC	plastocyanin
PCNA	proliferating cell nuclear antigen
PCR	polymerase chain reaction
PDB	Protein Data Bank
PDC	pyruvate dehydrogenase multienzyme complex
PDE	phosphodiesterase
PDGF	platlet-derived growth factor
PDI	protein disulfide isomerase
PE	phosphatidylethanolamine
PEP	phosphoenolpyruvate
PEPCK	PEP carboxykinase
PFGE	pulsed-field gel electrophoresis
PFK	phosphofructokinase
PG	prostaglandin
2PG	2-phosphoglycerate
3PG	3-phosphoglycerate
PGI	phosphoglucose isomerase
PGK	phosphoglycerate kinase
PGM	phosphoglycerate mutase
PH	phenylalanine hydroxylase *or* pleckstrin homology
Pheo	pheophytin
PhK	phosphorylase kinase
PIC	preinitiation complex
PI3K	phosphoinositide 3-kinase
PIP_2	phosphatidylinositol-4,5-bisphosphate
PK	pyruvate kinase
PKA	protein kinase A
PKB	protein kinase B
PKC	protein kinase C
PKU	phenylketonuria
PLC	phospholipase C
PLP	pyridoxal-5′-phosphate
pmf	protonmotive force
PMP	pyridoxamine-5′-phosphate
PNP	purine nucleotide phosphorylase
Pol	DNA polymerase
PP1	phosphoprotein phosphatase-1
PP_i	pyrophosphate ion
PPI	peptidyl prolyl cis–trans isomerase
PrP	prion protein
PRPP	5-phosphoribosyl-α-pyrophosphate
PS	photosystem
PtdIns	phosphatidylinositol
PTK	protein tyrosine kinase
PTP	protein tyrosine phosphatase
Q	ubiquinone (CoQ) or plastoquinone
QH_2	ubiquinol
QSAR	quantitative structure–activity relationship
r	ribo
RC	photosynthetic reaction center
RER	rough endoplasmic reticulum
RF	release factor *or* replicative form
RFLP	restriction-fragment length polymorphism
RK	HMG-CoA reductase kinase
RNA	ribonucleic acid
RNAi	RNA interference
RNAP	RNA polymerase
RNR	ribonucleotide reductase
R5P	ribose-5-phosphate
RPC	reverse phase chromatography
RRM	RNA-recognition motif
rRNA	ribosomal RNA
RS	tRNA synthetase
RSV	Rous sarcoma virus
RT	reverse transcriptase
RTK	receptor tyrosine kinase
RuBisCO	ribulose-1,5-bisphosphate carboxylase–oxygenase
RuBP	ribulose-1,5-bisphosphate
Ru5P	ribulose-5-phosphate
S	Svedberg unit
SAM	*S*-adenosylmethionine
SAR	structure–activity relationship
SCAP	SREPB cleavage-activating protein
SCID	severe combined immunodeficiency disease
SDS	sodium dodecyl sulfate
SH2	Src homology domain 2
SH3	Src homology domain 3
siRNA	small interfering RNA
SNAP	soluble NSF attachment protein
SNARE	SNAP receptor
snoRNA	small nucleolar RNA
snRNA	small nuclear RNA
snRNP	small nuclear ribonucleoprotein
SOD	superoxide dismutase
S7P	sedoheptulose-7-phosphate
SR	SRP receptor
SRE	sterol regulatory element
SREBP	SRE binding protein
SRP	signal recognition particle
SSB	single-strand binding protein
ssDNA	single-stranded DNA
STAT	signal transducer and activator of transcription
STC	sequence-tagged connector
STS	sequence-tagged site
SV40	simian virus 40
T	thymine
TAF	TBP-associated factor
TBP	TATA box-binding protein
TBSV	tomato bushy stunt virus
TCA	tricarboxylic acid
TGN	trans Golgi network
THF	tetrahydrofolate
TIM	triose phosphate isomerase
TLC	thin layer chromatography
TM	transmembrane
TMV	tobacco mosaic virus
topo	topoisomerase
TPP	thiamine pyrophosphate
tRNA	transfer RNA
TS	thymidylate synthase
TTP	thymidine triphosphate
U	uracil
UCP	uncoupling protein
UDP	uridine diphosphate
UDPG	uridine diphosphate glucose
UMP	uridine monophosphate
UTP	uridine triphosphate
UV	ultraviolet
V_{max}	maximal velocity
VLDL	very low density lipoprotein
XMP	xanthosine monophosphate
XP	xeroderma pigmentosum
Xu5P	xylulose-5-phosphate
YAC	yeast artificial chromosome
YADH	yeast alcohol dehydrogenase